JCTC
Journal of Chemical Theory and Computation
March 2011 Volume 7 Number 3 pubs.acs.org/JCTC

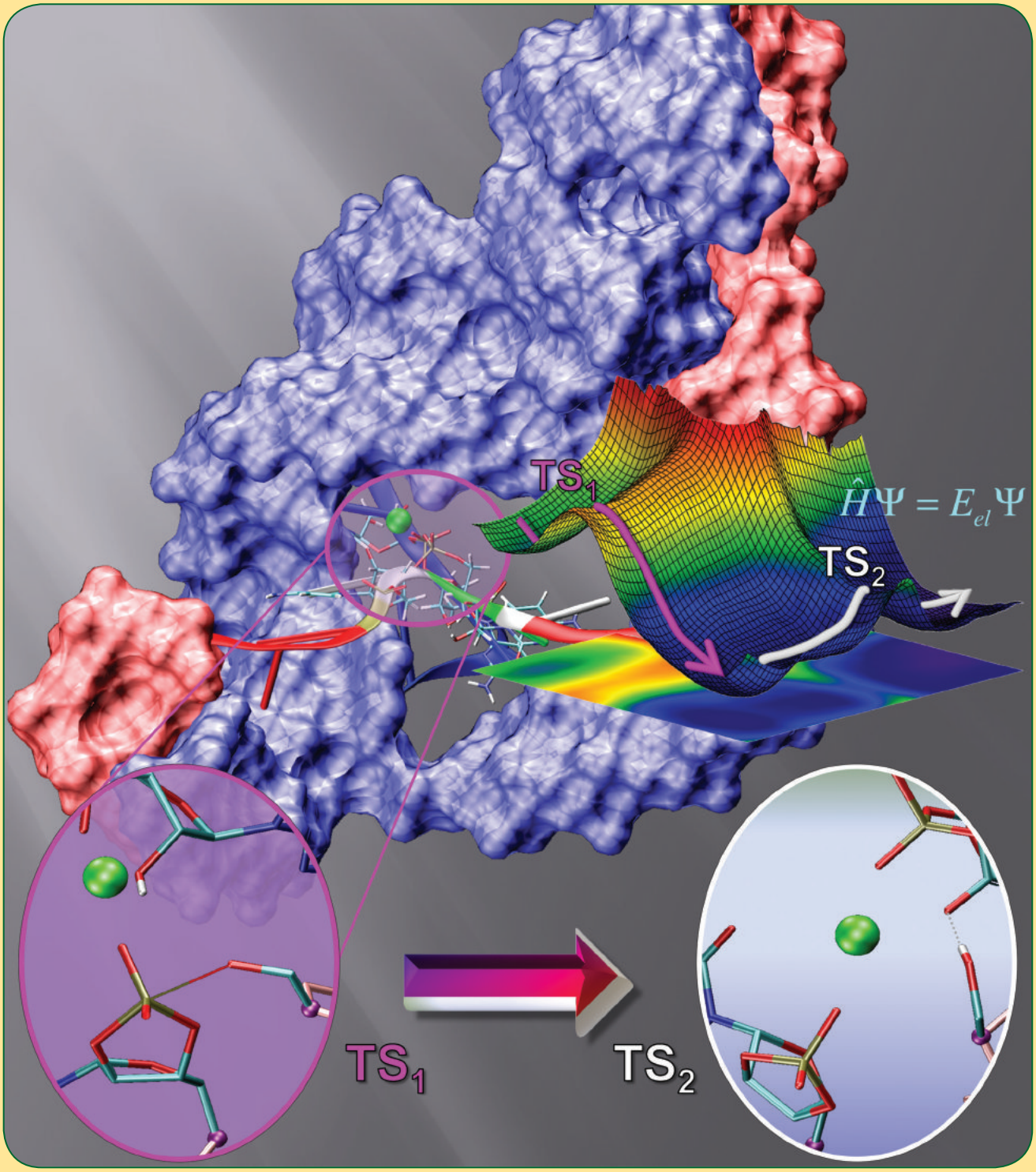

JCTC Journal of Chemical Theory and Computation

Active Participation of the Mg^{2+} Ion in the Reaction Coordinate of RNA Self-Cleavage Catalyzed by the Hammerhead Ribozyme

Kin-Yiu Wong,[†] Tai-Sung Lee,[‡] and Darrin M. York*[,†,‡]

Department of Chemistry, University of Minnesota, 207 Pleasant St. SE, Minneapolis, Minnesota 55455, United States, and BioMaPS Institute and Department of Chemistry and Chemical Biology, Rutgers, The State University of New Jersey, 610 Taylor Rd., Piscataway, New Jersey 08854-8087, United States

Received August 24, 2010

Abstract: We report results from combined quantum mechanical/molecular mechanical (QM/MM) free energy simulations to explore metal-assisted phosphoryl transfer and general acid catalysis in the extended hammerhead ribozyme. The mechanisms considered here assume that the 2′OH group of C17 has already been activated (i.e., is deprotonated) and acts as a nucleophile to go on an in-line attack to the adjacent scissile phosphate, passing through a pentavalent phosphorane intermediate/transition state, followed by acid-catalyzed departure of the O5′ leaving group of C1.1. A series of six two-dimensional potential of mean force profiles are reported in this study, requiring an aggregate of over 100 ns of QM/MM simulation. The simulations employ the AM1/d-PhoT semiempirical quantum model and linear-scaling QM/MM-Ewald method and explore mechanistic pathways for the self-cleavage. Results support the plausibility of a cleavage mechanism where phosphoryl transfer and general acid catalysis are stepwise, and where the catalytic divalent metal ion plays an active role in the chemical steps of catalysis.

Small self-cleaving ribozymes such as the hammerhead ribozyme (HHR) have been instrumental as model systems for RNA catalysis.[1−3] Recently, an extended HHR structure was determined by X-ray crystallography at 2.0 Å resolution,[4] in which a divalent metal ion was observed near the active site. Subsequent computer simulations lend credence to the possibility that this metal ion may play an active role in catalysis,[4,5] although free energy profiles to elucidate specific pathways have not yet been reported.

We report results from combined quantum mechanical/molecular mechanical (QM/MM) free energy simulations to explore metal-assisted phosphoryl transfer and general acid catalysis in the extended HHR. The mechanisms considered here assume that the 2′OH group of C17 has already been activated (i.e., is deprotonated) and acts as a nucleophile to go on an in-line attack to the adjacent scissile phosphate, passing through a pentavalent phosphorane intermediate/transition state, followed by acid-catalyzed departure of the O5′ leaving group of C1.1. The general acid is assumed to be the 2′OH group of G8.[6−8]

A series of six 2D potential of mean force (PMF) profiles is herein reported, requiring an aggregate of over 100 ns of QM/

Table 1. Relative Free Energies and Internuclear Distances at Various States of RNA Self-Cleavage Catalysis in Hammerhead Ribozymes[a]

	react	TS_1	int	TS_2	prod
Nu−P	3.50(04)	1.76(05)	1.66(03)	1.67(03)	1.68(03)
P−Lea	1.65(03)	2.11(05)	4.51(04)	4.24(48)	3.63(23)
gA−H	0.96(00)	0.96(00)	0.96(00)	1.78(04)	3.75(04)
H−Lea	2.57(51)	4.07(47)	4.13(73)	1.04(03)	1.00(03)
Mg^{2+}−Lea	3.99(18)	3.61(17)	2.02(05)	2.83(86)	4.48(05)
Mg^{2+}−gA	4.56(18)	4.03(18)	4.33(06)	3.38(86)	2.03(05)
ΔG	0.0(4)	24.4(6)	−6.7(3)	13.7(7)	−13.6(9)

[a] Free energies (ΔG) are in kcal/mol, which were extracted from 1D PMF profiles along the minimum free-energy path through the 2D profiles. Average distances (X−Y) are in Å. Standard deviations are listed in parentheses divided by the decimal precision of the average values. The abbreviations "react", "TS", "int", and "prod" signify reactant, transition, intermediate, and product states, respectively, and for the distance metrics, "Nu", "Lea", "gA", and "H" refer to the O2′ nucleophile, O5′ leaving group, general acid residues G8:O2′, and H2′, respectively.

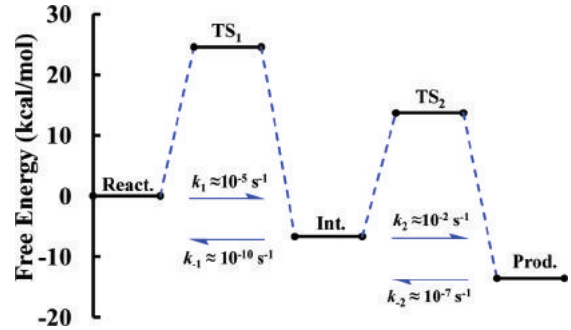

Figure 1. Schematic diagram for relative free-energy barriers and the corresponding reaction rate constants.

* Corresponding author e-mail: york@biomaps.rutgers.edu.
[†] University of Minnesota.
[‡] Rutgers University.

10.1021/ct100467t
Published on Web 12/16/2010

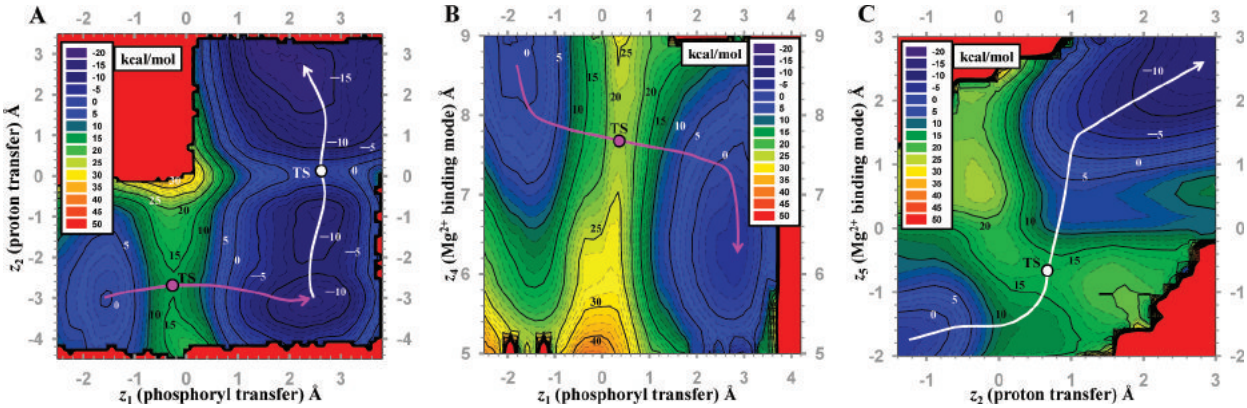

Figure 2. (A) Selected 2D surface, harmonically restrained along the course-grained metal ion binding coordinate at d (Mg^{2+}, G8:O2′) = 2.5 Å, where $z_1 = d$(O5′,P) − d(P,O2′), $z_2 = d$(G8:O2′,H) − d(H,O5′). (B) 2D PMF for the Mg^{2+} binding mode in the phosphoryl transfer step, where $z_4 = d$(Mg^{2+}, O5′) + d(Mg^{2+}, G8:O2′). (C) 2D PMF for the Mg^{2+} binding mode in the general acid step, where $z_5 = d$(Mg^{2+}, O5′) − d(Mg^{2+}, G8:O2′). $d(x,y)$ denotes distance between x and y. TS is the acronym of transition state.

MM simulation. Simulations were based on the extended HHR solvent structure (PDB: 2OEU)[4] solvated by over 10 000 water molecules. Active site residues (G8, A9, C1.1, C17, and an Mg^{2+} ion with coordinated water molecules shown in Figure 3) were treated quantum mechanically (81 atoms total) using the AM1/d-PhoT quantum model[9] with the AM1/d model for Mg^{2+}.[10] We used the all-atom AMBER parmbsc0 force field,[11] to describe the HHR outside of the active site, along with the TIP4P-Ewald water model[12] and the consistent set of monovalent ion parameters.[13] Multidimensional PMF profiles were generated along reaction coordinates corresponding to phosphoryl transfer, proton transfer from the general acid to the leaving group, and the divalent metal ion binding mode. Complete details are given in the Supporting Information.

Phosphoryl transfer and general acid steps are stepwise, and sensitive to the Mg^{2+} binding mode. Our initial attempts to study the chemical steps of the HHR reaction from 2D PMF profiles using phosphoryl transfer and proton transfer reaction coordinates, but not considering a reaction coordinate associated with Mg^{2+} ion binding mode, led to free energy barriers that were unexpectedly high (∼37 kcal/mol) compared to an estimated barrier of ∼20 kcal/mol derived from the experimental rate of one turnover per minute in HHR catalysis.[14] We extended the calculations so as to include a 3D-PMF profile with a course-grained reaction coordinate associated with the Mg^{2+} binding mode and confirmed the sensitivity of the barriers to the Mg^{2+} ion position along the reaction coordinate. A common feature of the reaction mechanism derived from the 3D profile was that the phosphoryl transfer and general acid steps were stepwise (e.g., Figure 2a), allowing these steps to be decoupled. Both the phosphoryl transfer and general acid steps of the reaction were coupled with the Mg^{2+} binding mode, and hence separate 2D profiles were generated for each step with a reaction coordinate corresponding to the Mg^{2+} binding mode as a second dimension. Table 1 summarizes key average geometrical parameters, and free energy values for stationary points along the reaction. The corresponding reaction rate constants are depicted in Figure 1.

Phosphoryl transfer is rate-limiting and facilitated by electrostatic stabilization by Mg^{2+}. The phosphoryl transfer step is rate-controlling, having a free energy barrier of approximately

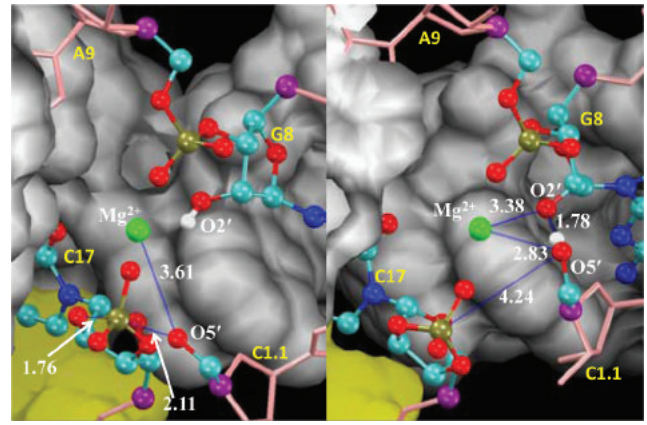

Figure 3. Snapshots of the active site at the transition states for phosphoryl transfer (left) and general acid catalysis (right) with average distances labeled.

24.4 kcal/mol. The position of the Mg^{2+} ion follows the negative charge along the phosphoryl transfer reaction coordinate in order to provide electrostatic stabilization. The change in the Mg^{2+} position is continuous and monotonic throughout the phosphoryl transfer step (Figure 2b) and is most pronounced in the initial and final stages when the nucleophile and leaving group have the greatest negative charge. The transition state is late (Figure 3), having a P−O5′ distance of 2.11 Å. As the P−O5′ bond breaks, the Mg^{2+} ion forms an innersphere coordination, leading to a Mg^{2+}-bound O5′ alkoxide intermediate.

General acid catalysis is concerted with changes in the Mg^{2+} binding mode. The general acid step considered here assumes that the 2′OH of G8 acts as a general acid catalyst to transfer a proton to the O5′ leaving group. An examination of Figure 2c indicates that proton transfer occurs after formation of the Mg^{2+}-coordinated cleaved intermediate and is concerted with changes in Mg^{2+} binding mode. Unlike the phosphoryl transfer step, participation of the Mg^{2+} along the reaction coordinate is most pronounced not at the end points of the step but near the midpoint where the proton transfer occurs.

The free energy barrier for the transition state of the general acid step (Figure 3) is 13.7 kcal/mol with respect to the activated precursor state. The intermediate is only 6.7 kcal/mol lower in

free energy than the activated precursor and has a 20.4 kcal/mol barrier to breakdown into the product state with a proton fully transferred to the O5′ leaving group.

Relation with experiment. The present work explores a specific mechanistic scenario, departing from the activated precursor state, that assumes the catalytic metal ion is in a position bridging the A9 and scissile phosphates, and the 2′OH of G8 acts as a general acid catalyst. The former metal ion binding mode has not yet been observed experimentally but has been inferred from biochemical experiments on the minimal[15] and extended[16] HHR and predicted by molecular simulations.[5,17,18] The latter role of G8 is consistent from structural[4] and biochemical data.[6−8] There has been seminal work on the study of metal ion interactions for the minimal HHR[19,20] that provide insight into the ligand environment of the site bound metal. Time-resolved NMR experiments suggest that there is a dynamic equilibrium between energetically similar conformations in the minimal HHR that are sensitive to Mg^{2+} binding,[21] and it has been suggested that the minimal and extended HHR may utilize a similar dynamic reaction mechanism for catalysis.[22] In the present study, we provide computational support for the plausibility of a cleavage mechanism where phosphoryl transfer and general acid catalysis are stepwise and the catalytic divalent metal ion plays an active role in the chemical steps of catalysis. It is the hope that this work, together with experimental work that probes the nature of metal ion interactions at the active site, will provide deeper insight into the underpinnings of chemical catalysis in the HHR.

Acknowledgment. The authors are grateful for financial support from the National Institutes of Health (GM084149 to D.Y.). Computational resources were provided by the Minnesota Supercomputing Institute (MSI) and by the NSF TeraGrid through the Texas Advanced Computing Center and National Institute for Computational Sciences under grant number TG-CHE100072. We thank Professor Victoria J. DeRose for useful comments on the manuscript.

Supporting Information Available: Additional computational details. This material is available free of charge via the Internet at http://pubs.acs.org.

References

(1) Strobel, S. A.; Cochrane, J. C. *Curr. Opin. Chem. Biol.* **2007**, *11*, 636–643.

(2) Scott, W. G. *Curr. Opin. Struct. Biol.* **2007**, *17*, 280–286.

(3) Leclerc, F. *Molecules* **2010**, *15*, 5389–5407.

(4) Martick, M.; Lee, T.-S.; York, D. M.; Scott, W. G. *Chem. Biol.* **2008**, *15*, 332–342.

(5) Lee, T.-S.; Silva Lopez, C.; Giambaşu, G. M.; Martick, M.; Scott, W. G.; York, D. M. *J. Am. Chem. Soc.* **2008**, *130*, 3053–3064.

(6) Blount, K. F.; Uhlenbeck, O. C. *Annu. Rev. Biophys. Biomol. Struct.* **2005**, *34*, 415–440.

(7) Nelson, J. A.; Uhlenbeck, O. C. *RNA* **2008**, *14*, 605–615.

(8) Thomas, J. M.; Perrin, D. M. *J. Am. Chem. Soc.* **2009**, *131*, 1135–1143.

(9) Nam, K.; Cui, Q.; Gao, J.; York, D. M. *J. Chem. Theory Comput.* **2007**, *3*, 486–504.

(10) Imhof, P.; Noé, F.; Fischer, S.; Smith, J. C. *J. Chem. Theory Comput.* **2006**, *2*, 1050–1056.

(11) Pérez, A.; Marchán, I.; Svozil, D.; Sponer, J.; Cheatham, T. E., III; Laughton, C. A.; Orozco, M. *Biophys. J.* **2007**, *92*, 3817–3829.

(12) Horn, H. W.; Swope, W. C.; Pitera, J. W.; Madura, J. D.; Dick, T. J.; Hura, G. L.; Head-Gordon, T. *J. Chem. Phys.* **2004**, *120*, 9665–9678.

(13) Joung, I. S.; Cheatham, T. E., III *J. Phys. Chem. B* **2008**, *112*, 9020–9041.

(14) Scott, W. G. What can the New Hammerhead Ribozyme Structures Teach us About Design? In *RNA Technologies and Their Applications*; Erdmann, V., Barciszewski, J., Eds.; Springer-Verlag: Berlin, Heidelberg, 2010.

(15) Wang, S.; Karbstein, K.; Peracchi, A.; Beigelman, L.; Herschlag, D. *Biochemistry* **1999**, *38*, 14363–14378.

(16) Osborne, E. M.; Schaak, J. E.; Derose, V. J. *RNA* **2005**, *11*, 187–196.

(17) Lee, T.-S.; Silva-Lopez, C.; Martick, M.; Scott, W. G.; York, D. M. *J. Chem. Theory Comput.* **2007**, *3*, 325–327.

(18) Lee, T.-S.; Giambaşu, G. M.; Sosa, C. P.; Martick, M.; Scott, W. G.; York, D. M. *J. Mol. Biol.* **2009**, *388*, 195–206.

(19) Vogt, M.; Lahiri, S.; Hoogstraten, C. G.; Britt, D. R.; DeRose, V. J. *J. Am. Chem. Soc.* **2006**, *128*, 16764–16770.

(20) Osborne, E. M.; Ward, W. L.; Ruehle, M. Z.; DeRose, V. J. *Biochemistry* **2009**, *48*, 10654–10664.

(21) Fürtig, B.; Richter, C.; Schell, P.; Wenter, P.; Pitsch, S.; Schwalbe, H. *RNA Biol.* **2008**, *5*, 41–48.

(22) Nelson, J. A.; Uhlenbeck, O. C. *RNA* **2008**, *14*, 43–54.

CT100467T